Prediction of CO_2 Corrosion for Welded Joints

by

Adzlan Bin Ayob

Dissertation submitted in partial fulfilment of
the requirements for the
Bachelor of Engineering (Hons)
(Mechanical Engineering)

JANUARY 2009

Universiti Teknologi PETRONAS
Bandar Seri Iskandar
31750 Tronoh
Perak Darul Ridzuan

CERTIFICATION OF APPROVAL

Prediction of CO_2 Corrosion for Welded Joints

by

Adzlan bin Ayob

A project dissertation submitted to the
Mechanical Engineering Programme
Universiti Teknologi PETRONAS
in partial fulfilment of the requirement for the
BACHELOR OF ENGINEERING (Hons)
(MECHANICAL ENGINEERING)

Approved by,

_____
(AP Ir. Dr. Mokhtar Che Ismail)

UNIVERSITI TEKNOLOGI PETRONAS

TRONOH, PERAK

January 2009

CERTIFICATION OF ORIGINALITY

This is to certify that I am responsible for the work submitted in this project, that the original work is my own except as specified in the references and acknowledgements, and that the original work contained herein have not been undertaken or done by unspecified sources or persons.

_____

(ADZLAN BIN AYOB)

ABSTRACT

Most CO_2 prediction models disregard the fact that the welded joints of pipelines are microstructurally different from the rest of the pipe material. The fact that the welded joints consist of different regions of microstructures indicates that they should behave differently due to the microstructure variation which then forms galvanic couplings. The aim of this research was to study the effect of different microstructure to the corrosion rate of welded A106 Grade B pipeline steel in 3% brines saturated with carbon dioxide at one bar pressure, under static condition, at a range of temperatures and also pH. Linear Polarization Resistance (LPR) technique is used to monitor the corrosion rate for each zone of the welds individually. The individual and galvanic corrosion rates for each of the weld region were measured electrochemically using the weld tester based on ZRA concept. The weld metal and HAZ were shown to be more anodic to the parent metal in pH 5 but there were some irregularities at high temperature and higher pH. The coupled HAZ and weld metal were found to be more anodic compared to the coupled HAZ and base metal thus showing the preferential weld corrosion at the weld metal and HAZ region. The galvanic effect between the microstructures is small since there are only slight microstructure differences between the regions. Findings showed that different microstructures of the different regions of the weld influenced the corrosion rates and also the preferential weld corrosion based on the LPR measurement and also galvanic current density measurement. Therefore it is concluded that the prediction models used to predict the corrosion rates of pipe line must consider the different regions of weld in its prediction.

ACKNOWLEDGEMENTS

First and foremost, the author would like to thank Allah, the Most Gracious *and* the Most Merciful for His blessings throughout the process of completion of this project.

The author would also like to express utmost gratitude to his supervisor, Assoc. Prof. Ir. Dr. Mokhtar Che Ismail, for the patience, advice, guidance and attention throughout the whole process of the project. Without the guidance and also the supervision, this project would not be possible to be completed successfully.

A special thank you to the following postgraduate students;Mr,Mohd. Faizairi Mohd.Nor,Ms. Anis Amilah Ab Rahman and Mr. Yuli Panca Asmara for their advices and also mentoring during the research period. Not to forget the Mechanical Laboratory Technicians especially Mr. M Faisal Ismail for his assistance at the corrosion laboratory in order to make the research a success. I am also grateful with the help from my friends especially Mr. Ameirul Azraie who had assisted me with thoughts and advices during the whole period of the project.

Not forgotten, lots of love to the author's parents, Mr. Ayob Bin Mohamed and Mrs. Siti Fatimah Binti Abdullah for their endless support and encouragement every single day which has driven the author to complete this project successfully.

Lastly, I would like to offer my regards and blessings to all of those who supported me in any respect during the completion of the project.

TABLE OF CONTENTS

LIST OF FIGURES

LIST OF TABLES

CHAPTER 1

INTRODUCTION

1.1 BACKGROUND OF STUDY

CO_2 corrosion is a common problem in the oil and gas industry [1-9]. Dry CO_2 is corrosive when it dissolves in an aqueous phase where it can promote an electrochemical reaction between steel and the contacting aqueous phase. Many reservoirs contains a significant amount of CO_2 which will then corrode the carbon steel used.

Most of pipelines used consist of many welded joints. The use of carbon steels in the pipelines of oil fields is mainly due to economic and strength reasons. Review of literature data and field experience indicate that preferential weld corrosion of pipe weldments is a problem of some concern to the oil and gas industry. There is also very little work related to the study of such corrosion problem has been reported. Apart from that, the understanding of many parameters such as temperature and also pH that may influence such corrosion is also limited.

The main cause of the preferential weld is due to the differential metallurgy and composition between the base metal and the weld metal .The microstructure of the metal is believed to have major influence on the corrosion rate in CO_2 environment [3, 4, 6, 7].Therefore a study on the affect of the different microstructures of the parent metal, weld metal and also the heat affected zone (HAZ) is done to obtain individual corrosion rates and the galvanic corrosion between the different regions of the weld.

1.2 PROBLEM STATEMENT

Corrosion failure of welds in CO_2 environment occurs despite the proper selection of the base metal and filler metal has been made, industry codes and standards have been followed. The importance of chemical compositions and also microstructure on CO_2 corrosion of carbon steels are highly recognized and many research have been done regarding that matter [12].Despite that, there are still uncertainties that can be found in other literature therefore it is a feasible for this project to be done in order to obtain results that will show the effects of the weld microstructures to the corrosion rate.

Most of the pipeline corrosion model and design assume that the pipes are seamless or homogenous. This is to simplify the corrosion prediction which does not include the welding zone of the pipelines which has different composition and microstructure due the effect of high temperature. However, the base metal or the parent metal, weld and also heat affected zone in real conditions experience different corrosion rate. Thus, understanding the effect of the different microstructures at different zone of the weld material to the corrosion rate for carbon steels in CO_2 environment at typical operating condition is needed.

1.3 SIGNIFICANCE OF THE PROJECT

During the late 1990's weld corrosion in CO_2 environment was observed on weldments in the oil and gas industry [4]. The different zones of weldments are susceptible to galvanic corrosion because of their compositional and also microstructural differences. Preferential weld corrosion has been found to be particularly problematic in oil and gas flow lines. Therefore, this project proposes to identify the uncertainties of the effect of the microstructures to the rate of weld corrosion of carbon steels by research and also experimental studies.

1.4 OBJECTIVE

The main objective for this project is to study the effect of different microstructure to the corrosion rate of welded A106B pipeline steel in brines saturated with carbon dioxide at one bar pressure, under static flowing conditions, at a range of temperatures and pH.

1.5 SCOPE OF STUDY

The scope of study is to focus on the difference of the microstructure of the different regions of the weld for different parts of the welded joints which is the:

- Base metal
- The heat-affected zone (HAZ)
- Weld metal

To conduct experiments based on the initial study of the microstructure to determine the influence of it to the rate of weld corrosion for carbon steels in CO_2 environments.

1.6 RELEVANCE OF THE PROJECT

The study of the affect of the microstructure to the rate of weld corrosion of carbon steels in CO_2 environments is very important especially in the oil and gas industry where all the pipelines and also process piping systems are affected by the weld corrosion. It has been increased in recent years. This project will present the result of the research done based on the laboratory experiments conducted on the corrosion rates for different segments of the weld in CO_2 environment.

1.7 FEASIBILITY OF THE PROJECT

The project will start with research on the microstructures and also the weld corrosion in CO_2 environments. The study will then focus on how the microstructures affects the rate of weld corrosion specifically for carbon steels in CO_2 environments .Then experiments will be done to get the actual results based on the earlier research.

CHAPTER 2

LITERATURE REVIEW

2.1 Corrosion in CO_2 Environments

In oil and gas industry, CO_2 is the main reason for corrosion to occur and the impact of the corrosion in oil and gas production and transportation facilities caused by CO_2 environments is very well recognized [3, 4].The problem of CO_2 corrosion has prompted a lot of studies in order to understand better on the mechanism of CO_2 corrosion.

CO_2 is not corrosive when it is in the dry gas state. Problem arises when the dry gas dissolved in an aqueous phase whereby an electrochemical reaction between the steel and aqueous phase will lead to corrosion. In the oil and gas industry, transportation facilities are the one facing the real problem due to the fact that CO_2 is extremely soluble in hydrocarbons and reservoirs usually contain a significant amount of CO_2 [10].

The presence of carbon dioxide will lead to the formation of a weak carbonic acid (H_2CO_3) which drives the CO_2 corrosion reactions. Carbonic acid or the bicarbonate ion formed by dissolution of CO_2 in water involves in all corrosion process. The process of corrosion is presented by the reaction shown in the equations as follows:

$$CO_{2\,(g)} + H_2O \rightarrow CO_{2\,(dissolved)} \quad (1)$$

$$CO_{2\,(dissolved)} + H_2O \leftrightarrow H_2CO_3 \leftrightarrow H^+ + HCO_3^- \quad (2)$$

The mechanism suggested by de Waard is:

$$H_2CO_3 + e^- \rightarrow H + HCO_3^- \quad (3)$$

$$2H \rightarrow H_2 \quad (4)$$

With the steel reacting:

$$Fe \rightarrow Fe^{2+} + 2e^{-} \quad (5)$$

The overall equation:

$$CO_2 + H_2O + Fe \rightarrow FeCO_3 \text{ (iron Carbonate)} + H_2 \quad (6)$$

It is stated that approximately 60% of oilfield failures are related to CO_2 corrosion mainly due to inadequate knowledge and also poor resistance of carbon alloy steels to this type of corrosive attack [5]. Apart from CO_2 corrosion, the metallurgy of the carbon steels is also important to have the understanding of the transformation during the welding process.

2.2 The Metallurgy of Carbon Steels

The best way to understand the metallurgy of carbon steel is to study the 'Iron Carbon Diagram'. The diagram shown below is based on the transformation that occurs as a result of slow heating. Slow cooling will reduce the transformation temperatures; for example: the A1 point also known as the eutectoid temperature would be reduced from 723°C to 690 °C. However the fast heating and cooling rates encountered in welding will have a significant influence on these temperatures, making the accurate prediction of weld metallurgy using this diagram difficult [11].

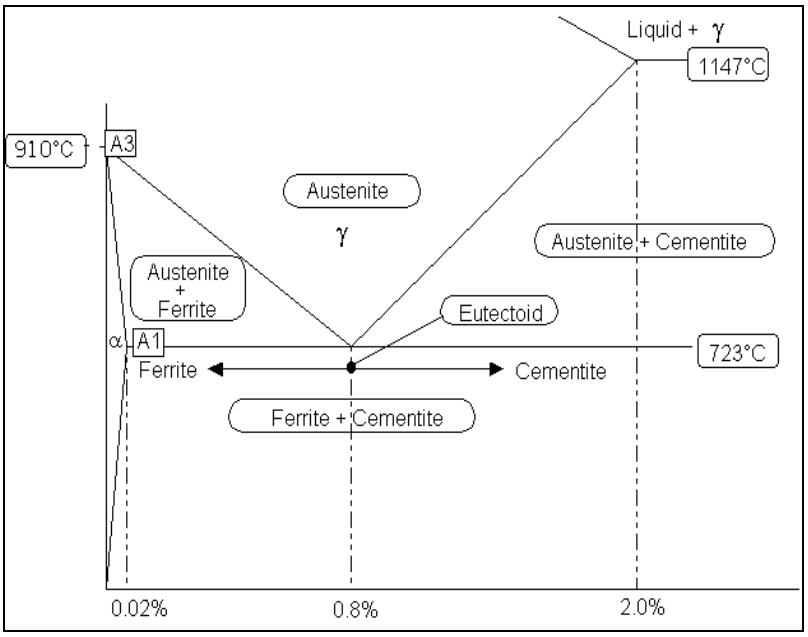

Figure 1: Iron Carbon Diagram

For cooling of steel below 0.8% carbon, the steel solidifies and forms austenite. When the temperature falls below the A3 point, grains of ferrite start to form. As more grains of ferrite start to form the remaining austenite becomes richer in carbon. At about 723°C the remaining austenite, which now contains 0.8% carbon, changes to pearlite. The resulting structure is a mixture consisting of white grains of ferrite mixed with darker grains of pearlite. Heating is basically the same thing in reverse. The phases present during the heating and cooling process are:

- **Austenite**

  This phase is only possible in carbon steel at high temperature. It has a Face Centre Cubic (F.C.C) atomic structure which can contain up to 2% carbon in solution[12].

- **Ferrite**

  This phase has a Body Centre Cubic structure (B.C.C) which can hold very little carbon; typically 0.0001% at room temperature. It can exist as either: alpha or delta ferrite [12].

- **Carbon**

  A very small interstitial atom that tends to fit into clusters of iron atoms. It strengthens steel and gives it the ability to harden by heat treatment. It also causes major problems for welding, particularly if it exceeds 0.25% as it creates a hard microstructure that is susceptible to hydrogen cracking. Carbon forms compounds with other elements called carbides such as iron carbide and chrome carbide.

- **Cementite**

  Unlike ferrite and austenite, cementite is a very hard intermetallic compound consisting of 6.7% carbon and the remainder iron, its chemical symbol is Fe_3C. Cementite is very hard, but when mixed with soft ferrite layers its average hardness is reduced considerably. Slow cooling gives course perlite; soft easy to machine but poor toughness. Faster cooling gives very fine layers of ferrite and cementite; harder and tougher.

- **Pearlite**

  Pearlite is a mixture of alternate strips of ferrite and cementite in a single grain [12]. The distance between the plates and their thickness is dependent on the cooling rate of the material where fast cooling creates thin plates that are close together and slow cooling creates a much coarser structure possessing less toughness. A fully pearlitic structure occurs at 0.8% Carbon. Further increases in carbon will create cementite at the grain boundaries, which will start to weaken the steel.

The differences between the phases of the weld metal based on the carbon steel diagram are believed to effect on the corrosion of the weld.

2.3 Microstructure and Corrosion

Studies have been done concerning the relation between microstructure of carbon steels to the corrosion in CO_2 environments. Past studies had shown that the microstructure of carbon steels are considered as an important factor and it has a significant influence to the CO_2 corrosion performance [6]. The impact of the carbon steel microstructure to the corrosion rate is also emphasized [5]. Consequently, experiments were conducted to monitor the corrosion performance of various grades of carbon steels in stirred autoclaves under elevated CO_2 and temperature conditions.

Samples were categorized to four groups based on their microstructure which is the banded ferrite/pearlite microstructure, very fine predominantly ferrite microstructures, coarser ferrite/acicular pearlite/pearlite microstructure and tempered martensite microstructure. It is clearly evident that based on the experiment done different groups of microstructures for the various carbon steels had given variations on the corrosion/penetration rate of the samples.

It was found that steels with a banded ferrite/pearlite structure perform poorly in terms of localized corrosion and this was attributed to a segregated distribution of the carbide phase cementite. Conclusion was made that steel microstructure is an important consideration when selecting pipe material for certain applications thus showing that microstructures do affect the corrosion performance of various carbon steels.

2.3.1 Weld Microstructure

Weldments exhibit special microstructural characteristics that have to be recognized and understood in order to predict tolerable corrosion service life of welded structures [2]. Weldments possess compositional and microstructural heterogeneities that can be classified by dimensional scale. A weldment normally consist of transition from the base metal through the HAZ and into the solidified weld metal and includes five microstructurally dissimilar regions known as the fusion zone, the unmixed region, the partially melted region, the HAZ and also the unaffected base metal.Not all of these zones are present in any given weldment.

If the temperature profile for a typical weld is plotted against the carbon equilibrium diagram as below, a wide range of transformation and heat treatments can be observed. The metallurgy of a weld is very different from the parent material. Welding filler metals are designed to create strong and tough welds, they contain fine oxide particles that permit the nucleation of fine grains. When a weld solidifies, its grains grow from the coarse HAZ grain structure. Further refinement takes place within these coarse grains creating the typical acicular ferrite formation shown opposite.

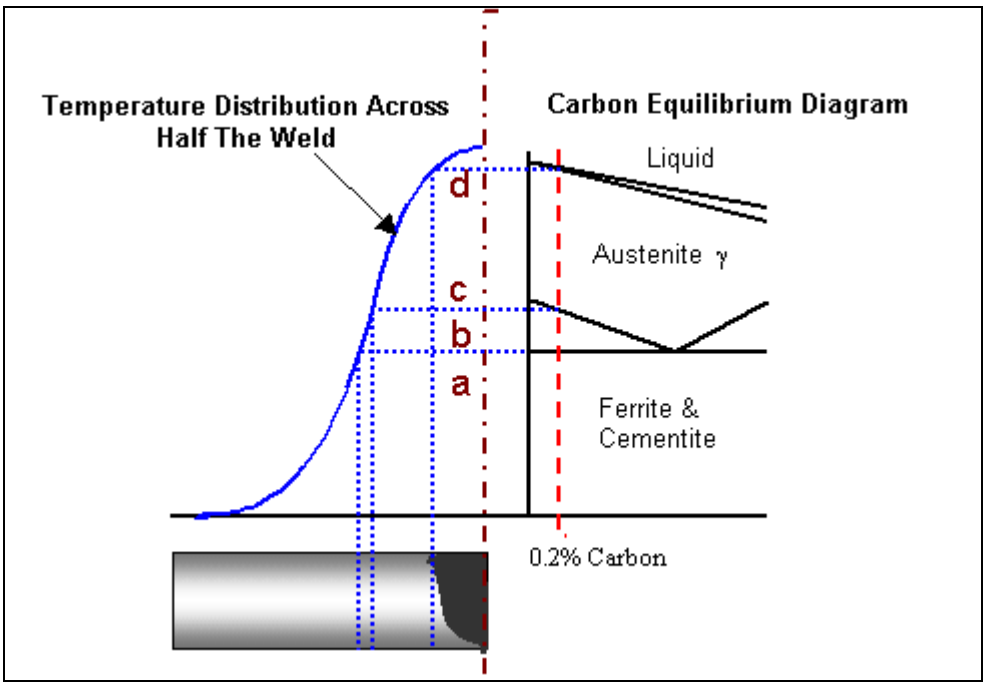

Figure 2: Temperature Distribution and the Carbon Equilibrium Diagram

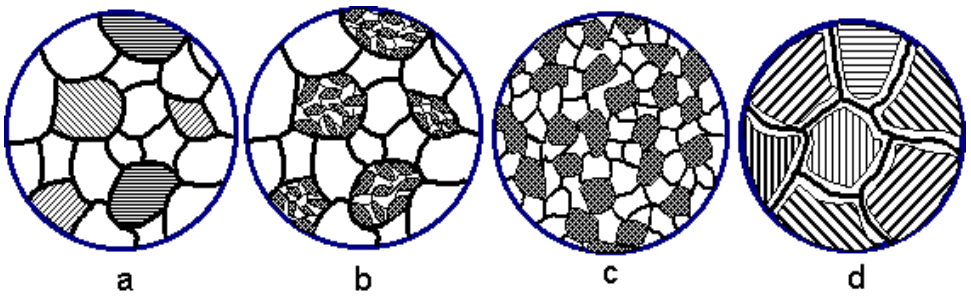

Figure 3 :Type of Microstructure phases

a. Mixture of ferrite and pearlite grains; temperature below A1, therefore microstructure not significantly affected.

b. Pearlite transformed to Austenite, but not sufficient temperature available to exceed the A3 line, therefore not all ferrite grains transform to Austenite. On cooling, only the transformed grains will be normalised.

c. Temperature just exceeds A3 line, full Austenite transformation. On cooling all grains will be normalised

d. Temperature significantly exceeds A3 line permitting grains to grow. On cooling, ferrite will form at the grain boundaries, and a course pearlite will form inside the grains. A course grain structure is more readily hardened than a finer one, therefore if the cooling rate between 800°C to 500°C is rapid, a hard microstructure will be formed. This is why a brittle fracture is most likely to propagate in this region.

The weld metal consists of 3 main regions which are the fusion zone,heat-affected zone(HAZ) and also the unaffected base metal. The fusion zone is the result of melting which fuses the base metal and filler metal to produce a zone with a composition that is most often different from the base metal [2]. The compositional variation produces a galvanic couple which can influence the corrosion process in the area of the weld. This dissimilar metal couple can produce macroscopic galvanic corrosion. The fusion zone undergoes microstructural segregation resulting from solidification therefore exposing it to microscopic galvanic effect.

The HAZ is the segment of the weld joint which has gone through peak temperatures high enough to generate solid-state microstructural changes but too low to cause any melting [2].Each position in the HAZ has its own microstructural features and corrosion susceptibility due to the difference of the thermal experience

at each point during the welding process in terms of maximum temperature and cooling rate. Microstructural gradients present along the HAZ due to different time-temperature cycles experienced by each elements [2].Normally the microstructures of the HAZ closest to the fusion zone will be coarse grain zone, followed by the intermediate grain zone and lastly fine grain zone. For this project the HAZ will only be considered as a single zone since the experiment will focus on the larger scale of microstructures.

The unaffected base metal is the part of the weld that has not undergone any metallurgical change but it is likely to be in a state of high residual stresses [2].

2.4 Preferential Weld Corrosion

Corrosion failure of welds is another well-known problem in the oil and gas industry. Even though lots of methods such as selecting the proper base metal and also filler metal and following industrial codes and standards, corrosion failure of welds still occur. In some cases, although the wrought form of a metal is resistant to the corrosion, the welded equivalent acts the other way around. There are also cases where welds with filler metals or even autogenous weld shows dissimilar corrosion behaviour between the weld and the unwelded base metal. Some weld exhibits corrosion resistance to the base metal but there are also times where weld behaves in an incoherent way displaying both resistance and also vulnerability to corrosive attack.

Location and morphology of the preferential corrosion is affected by a complex interaction of many parameters such as the environment, parent steel composition, weldment design, fabrication technique, porosity, cracks and many more. Changes in any of these factors may result in a major dissimilarity in the weldment corrosion behaviour [7]. Apart from that, metallurgical factors due to the constant exposure to high temperatures during the welding process affect the microstructure and also the surface composition of welds and the nearest base metal. Therefore corrosion resistance of the welds may be poorer than the base metal because of factors like microsegragation, recrystallization and grain growth in the weld HAZ,and also formation of unmixed zone, just to name a few.

Weldments are at risk to corrosion related with microstructure and composition such as galvanic corrosion, pitting, stress corrosion, intergranular corrosion, hydrogen cracking and also microbiologically influenced corrosion. This type of corrosion must be well thought-out when designing welded structures. More information on the topic of forms of weld corrosion can be found at the stated literature [3].

2.5 Microstructure and Preferential Weld Corrosion

Weld corrosion of carbon and low alloy steels used for pipelines and process piping systems in CO_2 environment still occur even after many studies have been made regarding this problem. Today, preferential weld corrosion of pipe weldments is a problem of some concern to the oil and gas industry. Weldments of any type is considered a complex metallurgical structure and the cause of the weldments corrosion is still being studied as there are many parameters that may influence the rate of the corrosion in CO_2 environments. It is predicted that the rate of weld corrosion is influenced by the microstructure of the welds and also parent metal.

The cycle of heating and cooling which occurs during the welding process affects the microstructure and also the surface composition for the weld and adjacent base metal. Because of that, the corrosion resistance of autogenous welds and welds made with matching filler metal may differ from the base metal due to the following reasons:

- Microsegregation
- Precipitation of secondary phase
- Formation of unmixed zones
- Recrystallization and grain growth in the heat-affected zone HAZ
- Volatilization of alloying elements from the molten weld pool
- Contamination of the solidifying weld pool

The results of a joint industry research program by three research organisations to investigate the effect of composition and microstructure on preferential weld corrosion in CO_2 media is presented by Lee,Bond and

Woolin[3].Twelve weld samples from X52 and X65 grade pipe materials with electrodes containing Ni or Cu were used to conduct the test. It was found that reasonable correlation between microstructure and preferential weld corrosion for weld metals. Weld metals with large unrefined ferrite with aligned second phase microstructures tend to give preferential weld metal corrosion while refined weld metals with less aligned second pHase ten to have similar corrosion rates to the parent steel.

Apart from that, it is obtained from the result that the weld metal corrosion increases as the hardness, grain size and also the level of aligned second phase increases. This supports to the earlier hypothesis of the study which states that the rate of weld corrosion is influenced by the microstructure of the weld and also base metal. One limitation to the study is that the relation between the heat affected zone (HAZ) corrosion with the HAZ hardness is not conclusive since the trend of the data obtained was not consistent thus further research on that relationship can be made to relate the hardness of the HAZ to the rate of corrosion.

In another literature by Andreassen and Enerhaug[9],reviews have been done on how the microstructure affects corrosion on carbon steel materials for top side production piping. Also included in the review are carbon steels and also pipe line materials. It is stated that in CO_2 corrosion of welds there is no common agreement on how different cementite forms influence the CO_2 corrosion. Several hypotheses from the literature survey were taken into account.

First hypotheses state that corrosion should be harsher in low temperature HAZs or with particulate cementite and corrosion will be less severe in areas with lamellar cementite. Second hypotheses stated that different ferrite structures will provide different persistence to the corrosion scale. Third hypotheses mentioned that ferrite should be more severely attacked and the last hypotheses stated that different fine grained structures of intragranular ferrite may render the weld metal and high temperature HAZ are more anodic.

After the metallurgical experiments were done, definite indications that the ferrite shape or grain sizes influence the corrosion rate are not found. Other than that, it is also still uncertain to relate that the rate of CO_2 corrosion for weld zones to specific microstructural constituents.

From the literature survey done on the affect of microstructures on CO_2 weld corrosion, it is found that there are still many uncertainties that need to be cleared. There are also few sources that specifically view on the affect of microstructures to the corrosion of weld in CO_2 environments thus there is a need to add researches and also studies to identify the solution or to understand this problem in the oil and gas industry.

2.6 Vickers hardness

The hardness test measures the resistance to the penetration of the surface of a material by a hard object. Hardness can represent the resistance to scratching or indentation and a qualitative measure of the strength of the material. Heat affected zone and the weld metal are hardened as a result of rapid heating and cooling.

Since cooling rate is high, considerable hardening occurs at the portion adjacent to the fusion line. The Vickers test uses a diamond pyramid indentor and it is suitable for materials that may have a surface that has different hardness at different areas in this case the difference of the microstructures between the different regions of the welded pipeline sample.

2.7 Linear Polarisation Resistance (LPR)

The electrochemical technique, commonly referred to as Linear Polarization Resistance, is the only corrosion monitoring method that allows corrosion rates to be measured directly, in real time. The polarizing voltage of 10 mV has been chosen as being well within the limits for which the linear relationship between I_{CORR} and $\Delta E/\Delta I$ holds. Additionally, the value is sufficiently small as to cause no significant or permanent disruption of the corrosion process, so that subsequent measurements remain valid. The procedures done are based on ASTM Standards [14-16].

Anodic and cathodic sites continually shift position, and they exist within a continuously conductive surface, making direct measurement of i_{corr} impossible. Small, externally-imposed, potential shifts (ΔE) will produce measurable current flow (ΔI) at the corroding electrode. The behaviour of the externally imposed current

is governed, as is that of i_{corr}, by the degree of difficulty with which the anodic and cathodic corrosion processes take place.

Therefore the greater difficulty will give smaller value of i_{corr} and ΔI for a given potential shift. In fact, at small values of ΔE, ΔI is directly proportional to i_{corr}, and hence to the corrosion rate. This relationship is embodied in the theoretically derived Stern-Geary equation:

$$\frac{\Delta E}{\Delta I} = \frac{\beta_a \beta_c}{2.3(i_{corr})(\beta_a + \beta_c)}$$

where βa and βc are the Tafel slopes of the anodic and cathodic reactions respectively.

CHAPTER 3

METHODOLOGY

The overall project flow chart is shown in Figure 4 .Research and study was on the first part of the project on journals and also technical papers that is related to the field of study. The second part of the project focuses more on the execution of the methodology in the labs and also obtaining the results which is then discussed later in the final report.

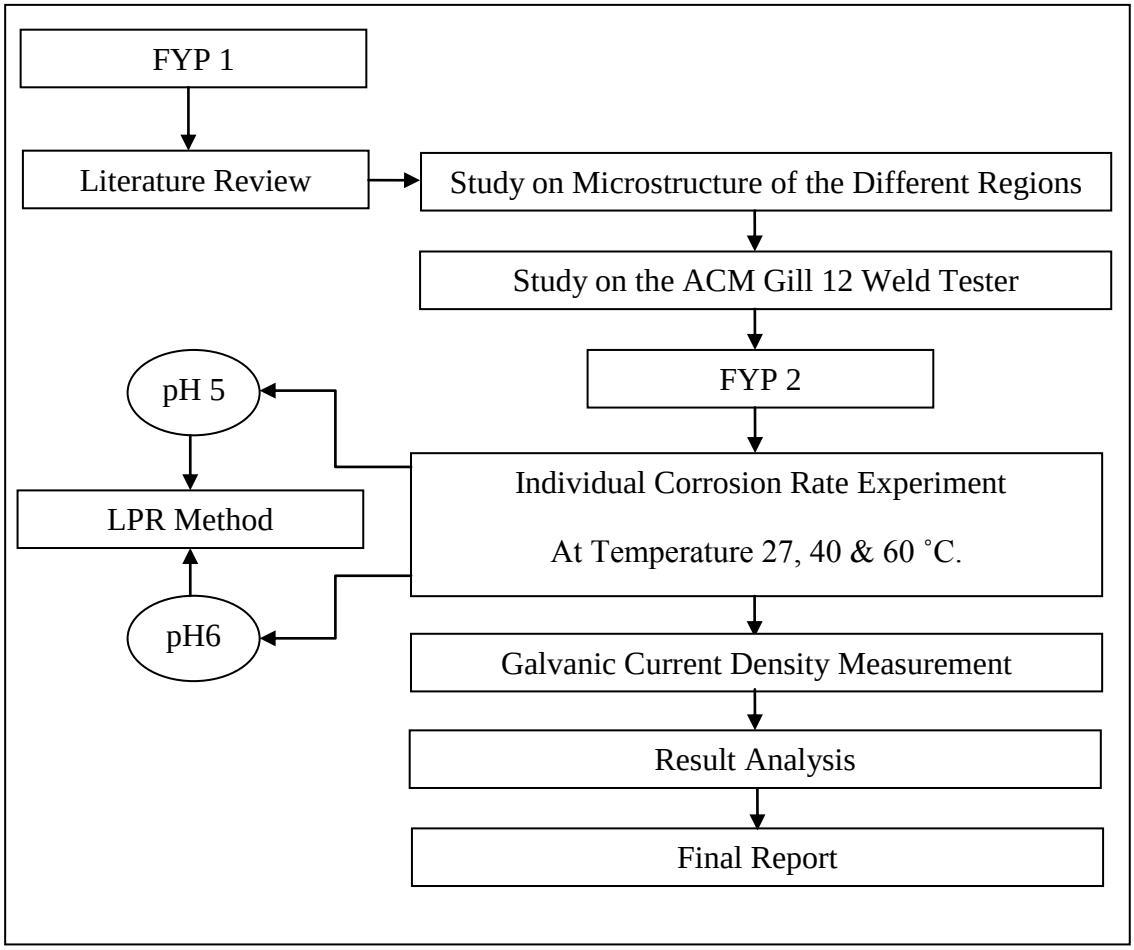

Figure 4: Project Flow Chart

The detail overview of the work flow for the whole project is available in Appendix 3-1 and Appendix 3-2.

3.1 Experiment Strategy

The objective of the experiment is to measure the corrosion rate, the mechanical properties and also characterization of the different region weld. Welds pose a particular problem because each weld is a complex galvanic couple made up of a parent metal, a weld metal and an area of heat affected metal. Under many circumstances the bulk of anodic dissolution is within the heat affected zone (HAZ).This very thin anode and large cathode of parent metal is the worst possible case rapidly leading to failure.

The solution is to segment the sample weld into 5 segments which are the Base Metal 1, the Haz 1, the Weld, the Haz 2 and also the Base Metal 2. The segmented pieces are then held on with epoxy. The instrument used to do this experiment is the weld tester. This instrument is a Gill 12 built to accommodate the extra four working electrodes per cell. Once the cell is connected the full range of tests are then used to determine the susceptibility of each component to the corrosion.

This potentiostat is particularly designed for measurements on galvanically coupled weld segments. Different type of measurements such as the Linear Polarization Resistance (LPR), Electrochemical Impedance Spectroscopy (EIS) and Potentiodynamic polarization measurements can be performed on each of the segments.

Linear Polarisation Resistance (LPR) method is used for this study and test was repeated at least two times to ensure the data acquired is accurate.

3.1.1 Vickers hardness test

The A106B weld sample is put under the test load of 300 gf and a dwell time of 15 seconds. Then under the 50x objective lens, the reading of the diamond shape at the material is taken. The test is done on the 5 different zones which is the base metal 1, heat affected zone 1, weld metal, heat affected zone 2 and the base metal.

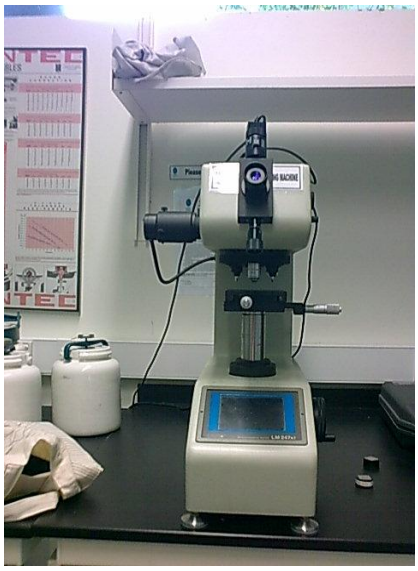

Figure 5: Micro hardness Testing Machine

3.1.2 Self Corrosion Rates

The self corrosion rates of each region were obtained by uncoupling the electrodes and measuring their polarization resistances by the linear polarization resistance technique. The potential of each weld component was scanned 10 mV above and below its open circuit value at a scan rate of 10 mV min^{-1} and the result was recorded. The polarization resistance, R_p was obtained from the best-fit gradient of the potential/current graph and the corrosion current i_{corr} was then found from the equation

$$i_{corr} = \frac{B}{R_p} \quad ; \; B = \frac{\beta_a \beta_c}{2.3(\beta_a + \beta_c)}$$

where B is a constant of the material. The value of B was taken as 25 mV. Due to the very small amount of potential range (10mV to -10mV) sweep, the polarization resistance method can be repeated over long periods without changing the behaviour of the sample. The self corrosion rates of the three weld regions are found after few runs of the experiment. Figure 5 shows the connection diagram for the self corrosion rates measurements.

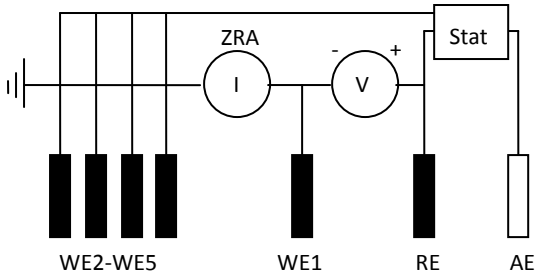

Figure 6: Connection Diagram for LPR Weld Corrosion Sweep

3.1.3 Galvanic Corrosion

Based on the result of the individual corrosion rates for pH 5 at which the most cathodic region is the base metal and the most anodic region is the weld metal, and the trend of the corrosion rate for the different temperatures are similar, the next step of the experiment was to conduct the galvanic corrosion analysis of the weld metal by coupling the different regions together.

Galvanic corrosion was simulated by electrically connecting:

a) Weld metal region with the HAZ region.
b) Base Metal region with the HAZ region.

The intention was to measure the galvanic current of the weld as a whole rather than individually and to recognize the cathodic or anodic region of the weld. Figure 6 shows the connection diagram for galvanic current density measurement where WE4 is coupled with WE5 and WE2 is coupled with WE3.

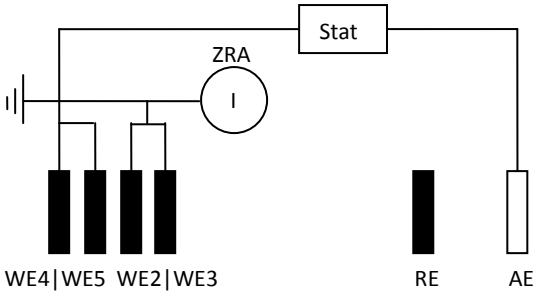

Figure 7: Connection Diagram for Galvanic Current Density Measurement

3.2 Sample preparation

3.2.1 Weld Characterization

Characterization of the microstructure in addition to corrosion were conducted in samples taken from the base metal and from the root and filler passes, in order to compare useful properties for the three weld regions. The three main regions of the weld which is the base metal, the heat affected zone (HAZ) and also the weld metal need to be identified by optical microscope and sample of each were machined to produce separate sample of different zones. Weld specimens were cut from pipe weld samples produced particularly for the project. Initially the weld metal is machined and then it will be grinded using the metallurgical grinder. Next, it will be polished using the metallurgical polisher.

Specimens were etched in Nital solutions to reveal the position of weld and HAZ zone. The purpose of these steps are to get the image of the microstructure of the weld metal using optical microscope and to distinguished the difference between the region of base metal, the heat affected zone and the weld metal. Figure 4 shows the sample of the weld and the regions. After that, the region is marked to divide them.

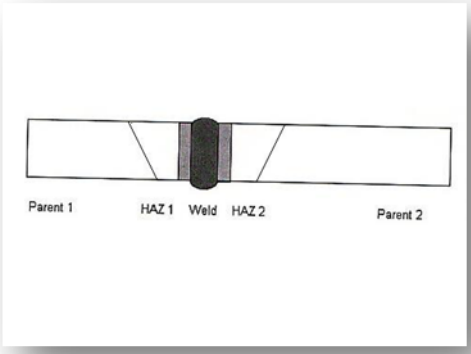

Figure 8: Weld Sample and its regions

A welding sample of A106 Grade B pipe sample was obtained and preparations were done to do initial study on the microstructures of the welded pipeline at the materials lab. This is because in order to observe the microstructures of the different zones in the weldment as shown in Figure 8, the sample must first be grinded and

also polished. An optical microscope is used to observe the microstructures of the welded pipeline as shown in Figure 9.

Figure 9: Optical Microscope

The sample was first cut using the abrasive cutter and was grinded using the metallurgical grinder. The metallurgical grinder was used to grind the surface of the weld so that the microstructure can be seen clearly using the optical microscope.

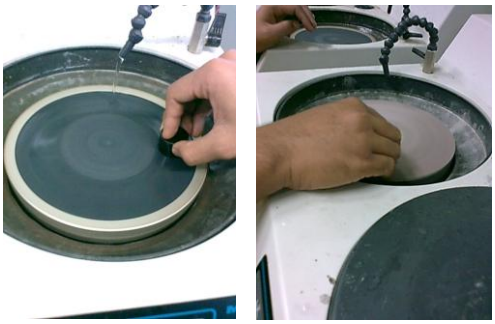

Figure 10: Metallurgical Grinder and Polisher

After grinding, then the sample is polished using the metallurgical polisher as shown in Figure 10. The sample is polished in 2 stages as follows: (1)6µm diamond suspension with blue lubricant,(2)1µm diamond suspension with blue lubricant. The polished sample was then etched in 2% nital (nitric acid in anhydrous methanol).Figure 11 shows the weld sample before and after grinding and polishing.

(a)  (b) 

Figure 11: Photographs taken of the weld sample (a) Weld sample before grinding and polishing and (b) Weld sample after grinding and polishing.

3.2.2 Corrosion Measurement

The different regions of weld metal is marked to a dimension of 0.5x1 cm to be machined later using the EDM machine.EDM machine is used to prevent heat build up at the cutting area that might influence the microstructure of the sample later. The different zones are differentiated using the optical microscope so that clear image of the microstructures can be obtained. Figure 12 shows the weld sample being marked .It is then being sent to be machined.

The weld sample is then machined using the EDM wire cutter .After finished cutting the weld sample, the five samples from different zone of the weld will be grinded and polished and rechecked using the optical microscope to make sure that the right zone is cut. After that, insulated copper wires are connected to each of the samples for electrical conductivity. The samples are then mounted together on epoxy for the next process which is determining the corrosion rate using the weld tester.

Figure 12: A106B steel weld marked for EDM cutting

After getting the sample back from the lab, each of the samples is then connected to the insulated copper wire by soldering it. After connecting the copper wire,

conductivity is then checked using the multimeter. The sample is then cold mounted using epoxy resin to complete the material preparation process.

Figure 13: Set-up for Cold Mounting

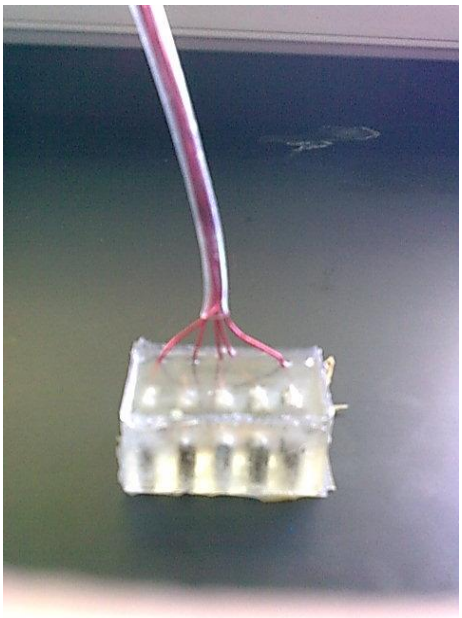

Figure 14: Sample after cold mounting showing Copper wire connection

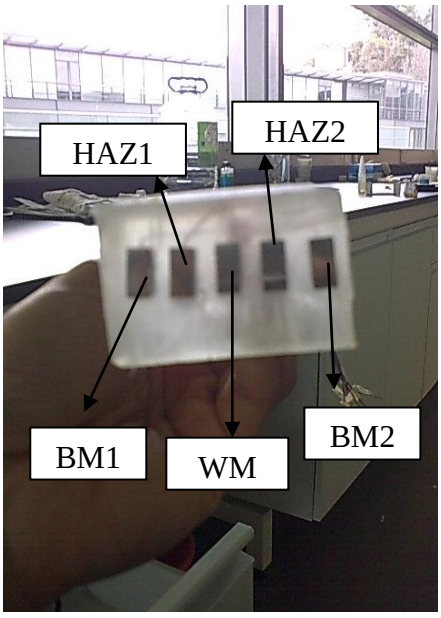

Figure 15: Bottom view of the sample showing the different weld regions

3.3 Experiment Setup

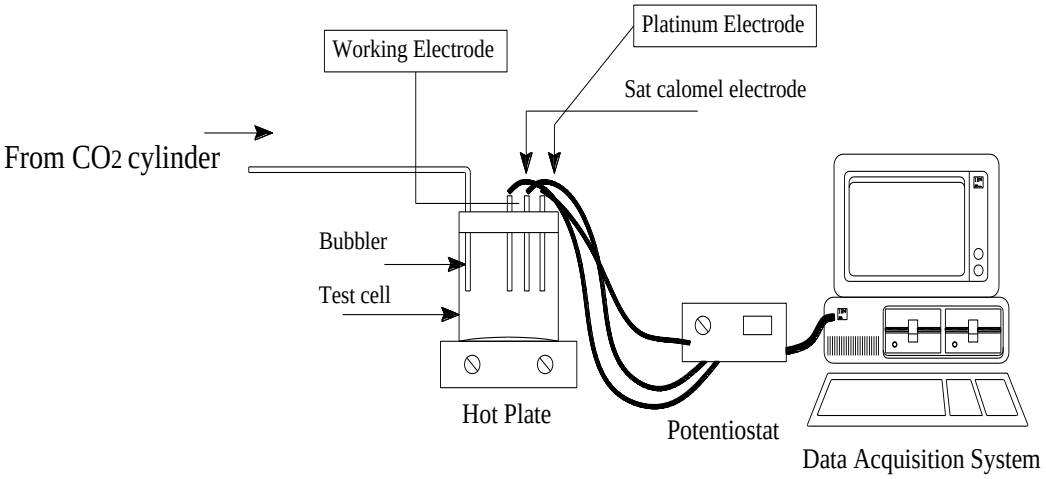

Figure 16 :Set-up for the experiment

Figure 16 shows the set-up for the experiment including the parent metals; BM1 & BM2, Heat-affected zone, HAZ1 & HAZ2; Reference Electrode, RE; Auxiliary Electrode, AE. The test matrix of the experiment is shown in Table 1. The test assembly consists of one-liter glass cell bubbles with CO_2. The required test temperature is set through a hot plate. The electrochemical measurements are based on a three-electrode system, using a commercially available potentiostat with a computer control system.

Table 1: Test matrix for the research

Parameter	**Value**
Steel Type	Carbon Steel, A 106B
Solution	3 % NaCl
De-oxygenation gas	CO_2
pH	5, 6
Temperature (°C)	27, 40, 60
Sand paper grit used	600,800,1200
Measurement techniques	Polarisation, LPR

3.4 Experimental Procedure

The experiment procedure is performed after the solution is saturated with CO_2 after the purging process, mixing the solution to the wanted pH and setting the solution to the working temperature. These are the normal experimental procedure for the individual corrosion rate measurement for both pH 5 and pH 6.

1. Purging the CO_2 through the 1-litre 3% NaCl for 1 hour
2. Solution of 1M $NaHCO_{3\ is}$ added to adjust pH to the required values. The pH of the solution is measured using the pH meter.
3. Set the temperature and maintain with an accuracy ±5°C.
4. Insert the specimen into the solution.
5. Take readings every 15 minutes for 1:30 hours.

The supply or bubbling of the CO_2 gas is maintained throughout the experiment.

For the Galvanic current measurement, same experimental procedure is applied but different settings of the weld tester are used compared to the normal LPR sweep for the individual corrosion rates.The self corrosion rate and the galvanic corrosion rates is then summed to obtain the total corrosion rate of the different regions:

Total Corrosion Rate = Self Corrosion Rate +Galvanic Corrosion Rate

The individual currents for the galvanic current density measurement from the coupled samples are established from the following relationship:

$$\mathbf{I_{BM} + I_{HAZ} + I_{WM} = 0}$$

CHAPTER 4
RESULTS AND DISCUSSION

The results obtained from the microstructure characterization, the Vickers hardness test, the self-corrosion rates and the galvanic current density measurement are discussed in this chapter.

4.1 Characterization of Weld Microstructure

The microstructures of the different regions for the weld steel pipeline sample are shown in Figures 17-20.Figure 17 shows the microstructure of the base metal region where the microstructure consists of pearlite and ferrite.The dark grains of the microstructure represents the pearlite grains while the bright grains represents the ferrite grains.The microstructure of the base metal region is not significantly affected since it is exposed to temperatures below A1,also known as the eutectoid temperature.

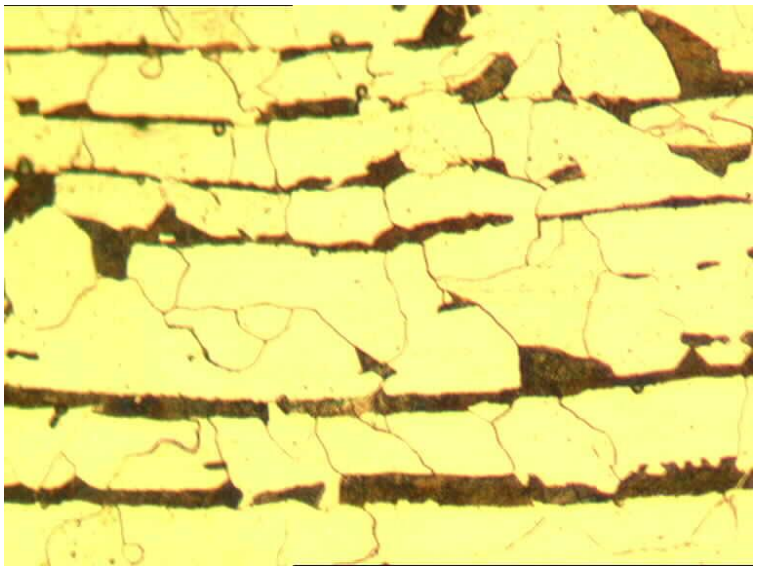

Figure 17: Base Metal microstructure for Welded A106B Pipeline Steel Sample (10µm)

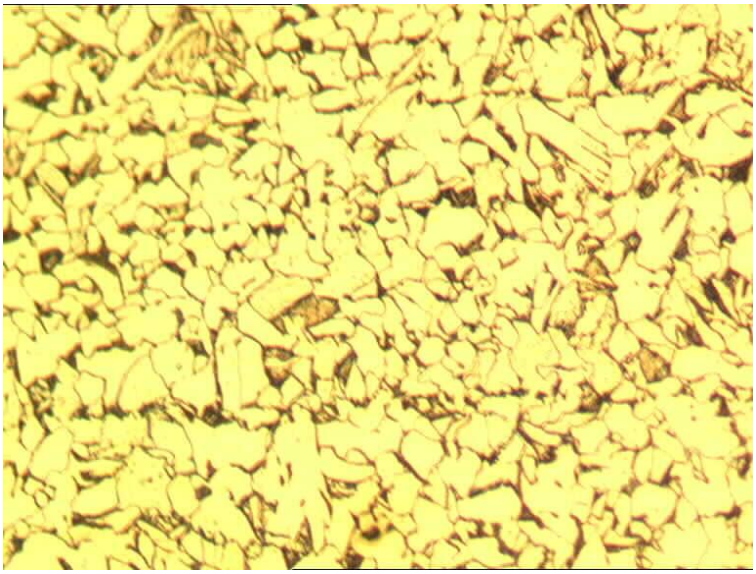

Figure 18: HAZ microstructure for Welded A106B Pipeline Steel Sample (10µm)

Figure 18 shows the microstructure for the Heat-Affected Zone, (HAZ) where it can be seen that the grains are transforming into a much softer matrix of ferrite and pearlite compared to the base metal microstructure earlier. This is because the HAZ segment has gone through high temperature which transforms the prior pearlite grains into austenite and expand slightly to prior ferrite upon heating and the decompose to extremely fine grains of pearlite and ferrite during cooling.

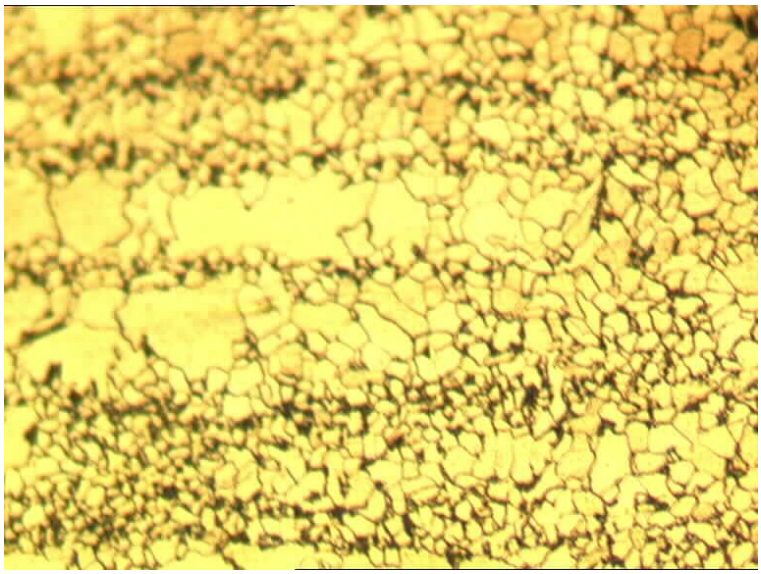

Figure 19: HAZ microstructure near Weld Metal Region for Welded

A106B Pipeline Steel Sample (10µm)

Longer exposure to higher temperature will then cause the austenite grains to decompose into non-uniform distribution of small ferrite and pearlite grains during cooling thus giving the grain-refining region as shown in Figure 19 where the transition of the different regions are clear. Apart from that it is known that HAZ closest to the fusion zone will be the coarse grain zone, followed by the intermediate grain zone and finally the fine grain zone.

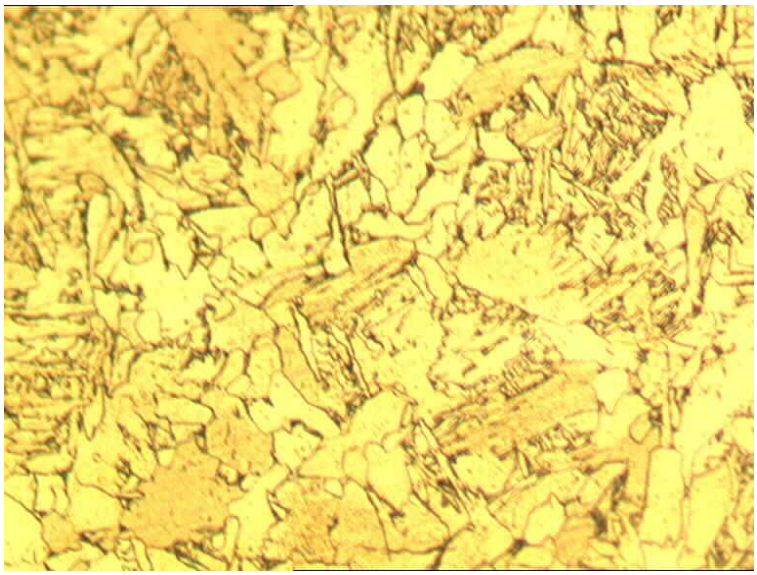

Figure 20: Weld Metal microstructure for Welded A106B Pipeline Steel (10µm)

The weld microstructure, as shown in Figure 20 shows the predominately acicular ferrite due to melting and solidification at high temperatures of the welding process (above the liquidus temperature). Acicular ferrite is desirable because it improves toughness of the weld metal in association with fine grain size therefore providing the maximum resistance to cleavage crack propagation.

It is established from the results obtained that there are variation in the size and type of the microstructure along the weldment zones due to the dissimilarities in experienced peak temperature or temperature distribution during the welding process which may affect the corrosion rate of the welded pipeline.

4.2 Vickers hardness Results

Table 2 shows the data obtained from the Vickers hardness test and the average reading for each zone plotted in Figure 21.

Table 2: Vickers Hardness (Hv) of the material at different zones

	Base Metal	**Heat-Affected Zone 1**	**Weld Metal**	**Heat-Affected Zone 2**	**Base Metal 2**
1	147.0	156.9	172.1	158.5	145.6
2	145.8	161.9	180.4	153.1	147.9
3	146.2	168.9	179.3	168.8	141.9
Average	**146.33**	**162.56**	**177.27**	**160.13**	**145.13**

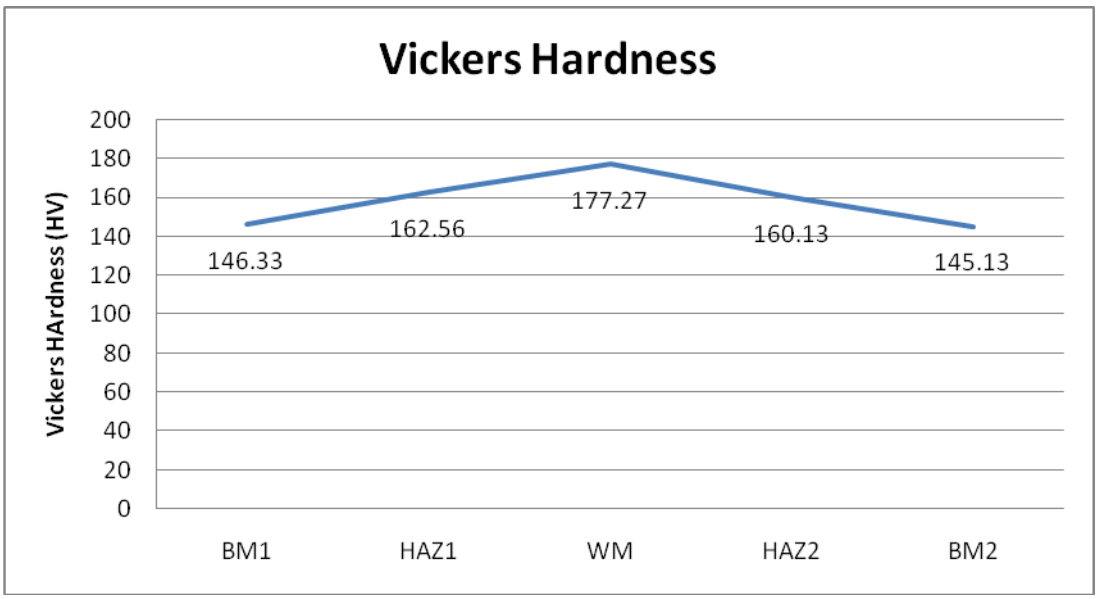

Figure 21: Hardness Distribution in weld of A106B steel

From the results obtained, it can be seen that the hardness of the metal is highest in the weld metal regions with 177.27 Hv , as compared to the heat affected zones ,HAZ 1 and HAZ2 with 162.56 Hv and 160.13 Hv respectively and finally both of the base metal with 146.33 Hv and 145Hv. From the result of the microstructure earlier, it can be related that the hardness of the weld region is the

highest due to the acicular ferrite form of the grains. Hardness of the material for the different microstructures from the different zones is needed to gain information regarding the mechanical properties for each zone and to show that it varies due to the difference in the microstructure.

4.3 Self-Corrosion Rate Results

The self corrosion rates of the three weld regions are found after repeated runs of the experiment.

4.3.1 Results for pH 5 at 27, 40 and 60 ˚C.

Table 3 shows the self corrosion rates from the linear polarization weld corrosion sweep at pH 5 for 90 minutes immersion in CO_2 saturated 3% NaCl solution at 27˚C.

Table 3: Self-Corrosion rate for blank pH 5 at 27 ˚C (CR-mm/yr)

No	**Z1**	**Z2**	**Z3**	**Z4**	**Z5**
	BM1	**HAZ1**	**WM**	**HAZ2**	**BM2**
1	0.86	1.36	1.41	1.20	1.06
2	0.85	1.37	1.38	1.19	1.01
3	0.87	1.38	1.39	1.19	1.03
4	0.87	1.36	1.39	1.17	1.05
5	0.88	1.35	1.39	1.21	1.06
Average	**0.87**	**1.36**	**1.39**	**1.19**	**1.04**

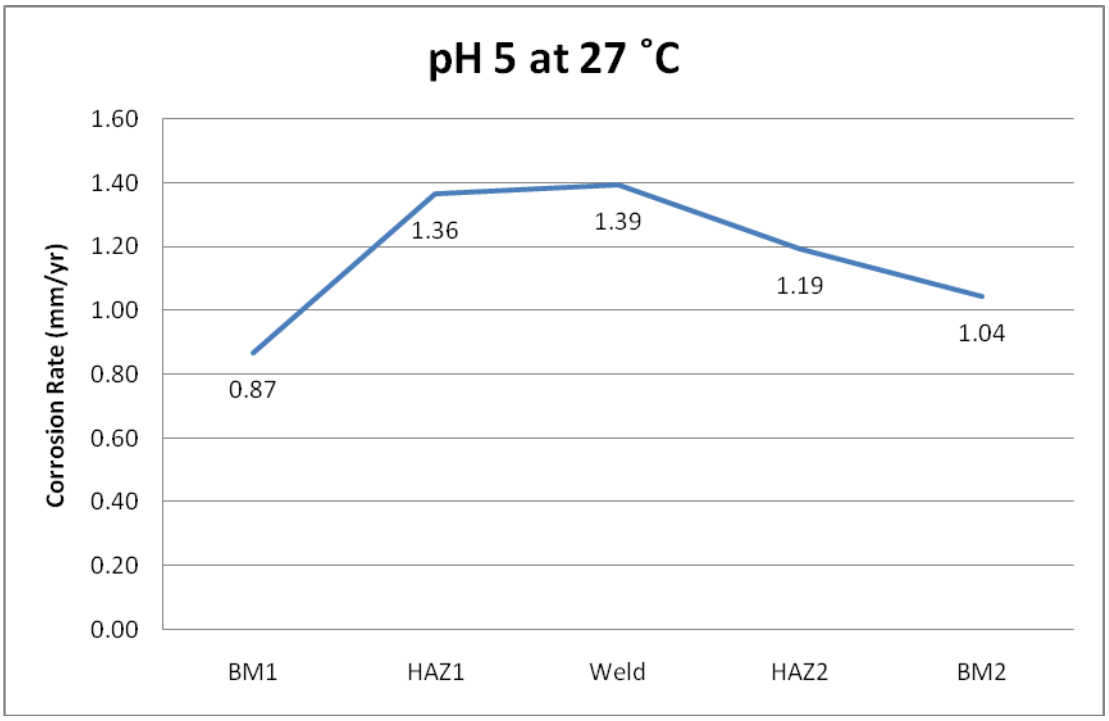

Figure 22: Corrosion Rate for different weld regions, pH 5 at 27 ˚C

The self corrosion rate at ambient temperature is as shown above. The corrosion rate of the weld metal region is the highest with 1.39 mm/yr followed by HAZ 1 with 1.36 mm/yr the HAZ2 region with 1.19 mm/yr and finally the base metal region, BM1 with 0.87 mm/yr and BM2 with 1.04 mm/yr. Although there are differences of the corrosion rate between the two HAZ regions, the corrosion rate is still below the weld metal's corrosion rate. Most probably the difference is caused by the irregularities of the microstructure between the regions. It is obtained from the results that the weld metal region and also the HAZs are more anodic compared to the base metal. The difference of the microstructure of the different region may have affected the corrosion rates of each of the region thus giving the undesired condition of anodic weld metal and HAZs.

Table 4 shows the self corrosion rates from the linear polarization weld corrosion sweep at pH 5 for 90 minutes immersion in CO_2 saturated 3% NaCl solution at 40˚C.

Table 4: Self-Corrosion rate for blank pH 5 at 40 ˚C (CR-mm/yr)

No	**Z1**	**Z2**	**Z3**	**Z4**	**Z5**
	BM1	**HAZ1**	**WM**	**HAZ2**	**BM2**
1	2.17	3.08	3.18	2.87	1.78
2	2.09	3.10	3.23	2.42	1.74
3	2.23	3.05	3.35	2.66	1.90
4	1.89	3.10	3.12	2.80	1.81
5	2.00	3.09	3.10	2.76	1.93
Average	**2.07**	**3.08**	**3.20**	**2.70**	**1.83**

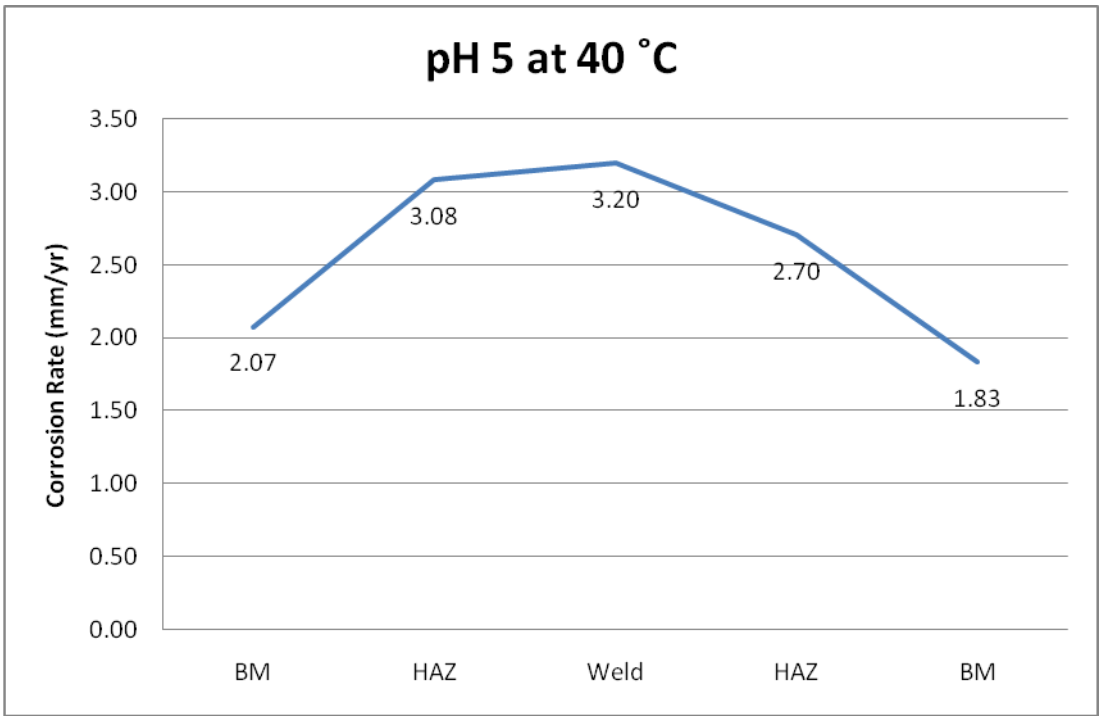

Figure 23: Corrosion Rate for different weld regions, pH 5 at 40 ˚C

The corrosion rates for the individual regions is obtained from the LPR test for pH 5 at 40˚C and the average of the corrosion rates are then plotted as in Figure 23 .It is

seen that the weld metal has the highest rate with 3.20 mm/yr followed by the HAZ ,HAZ1 with 3.08 mm/yr and HAZ2 with 2.70 mm/yr and finally the base metal, BM1 with 2.07mm/yr and BM2 with 1.83 mm/yr. Similar trend of corrosion rate is shown here compared to the experiment done at ambient temperature. However, the data indicates that the corrosion rates are slightly higher than the weld at ambient temperature. This indicates the effect of temperature to the corrosion rates of the weld sample. It is also shown that there are still differences between the corrosion rates of the HAZ region but it is still less anodic compared to the weld metal.

Table 5 shows the self-corrosion rates from the linear polarization weld corrosion sweep at pH 5 for 90 minutes immersion in CO_2 saturated 3% NaCl solution at 60˚C.

Table 5: Self-Corrosion rate for blank pH 5 at 60 ˚C (CR-mm/yr)

No	**Z1**	**Z2**	**Z3**	**Z4**	**Z5**
	BM1	**HAZ1**	**WM**	**HAZ2**	**BM2**
1	2.65	3.60	3.73	3.55	2.44
2	2.76	3.72	3.77	3.50	2.56
3	2.58	3.44	3.66	3.40	2.28
4	2.57	3.88	3.87	3.32	2.31
5	2.36	3.41	3.50	3.35	2.28
Average	**2.58**	**3.61**	**3.71**	**3.42**	**2.37**

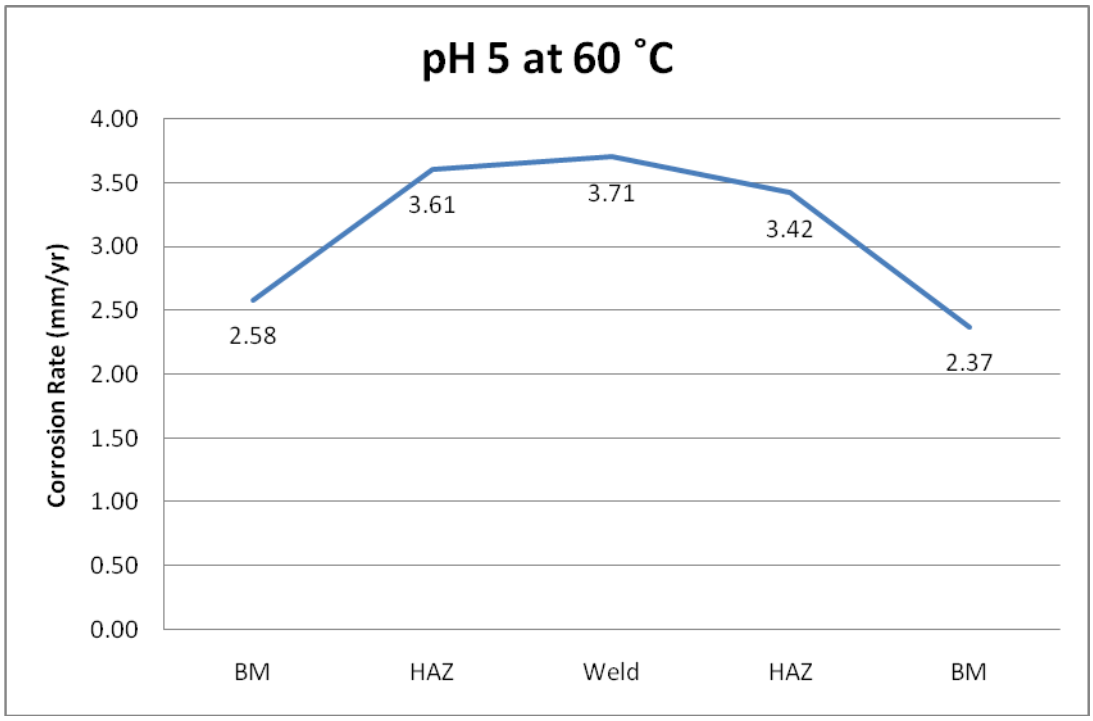

Figure 24: Corrosion Rate for different weld regions, pH 5 at 60 ˚C

The experiment at final temperature for the pH 5, which is at 60 ˚C, is shown tabulated in Table 5 above and the average corrosion rate is as shown in Figure 24. Similar as both of the temperatures before, the weld metal has the highest corrosion rate with 3.71 mm/yr followed by HAZ2 and HAZ1 with 3.61 mm/yr and 3..42 mm/yr respectively and finally the BM1 with 2.58 mm/ye and BM2 with 2..37 mm/yr. This gives the weld metal to be more anodic compared to the base metal.

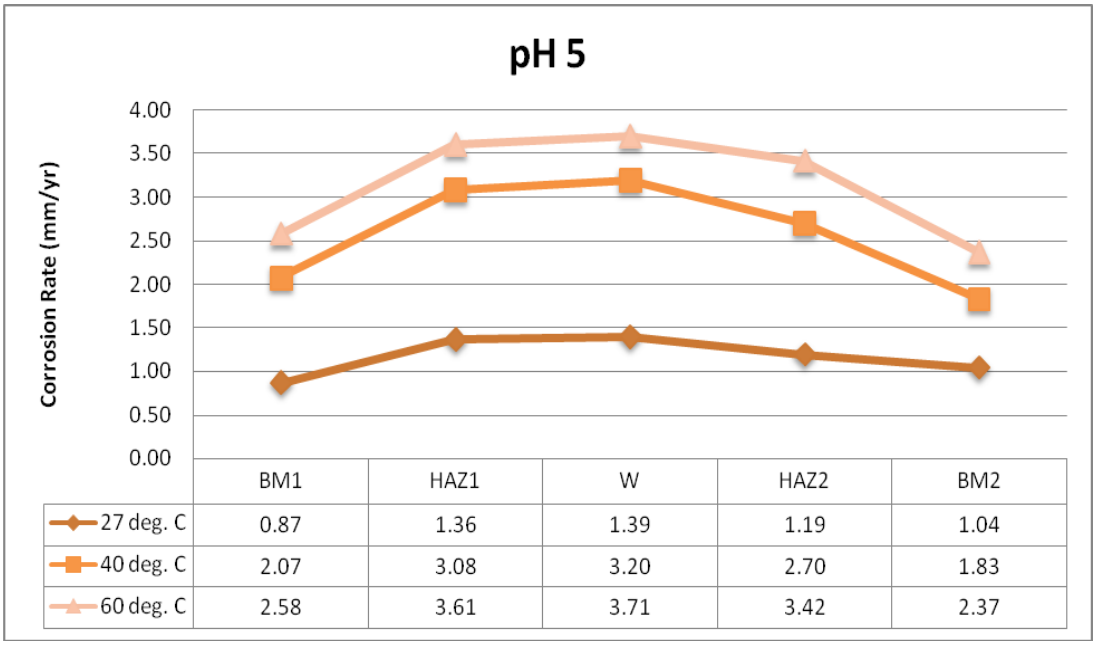

	BM1	HAZ1	W	HAZ2	BM2
27 deg. C	0.87	1.36	1.39	1.19	1.04
40 deg. C	2.07	3.08	3.20	2.70	1.83
60 deg. C	2.58	3.61	3.71	3.42	2.37

Figure 25: Comparison of Corrosion Rate for pH 5 at Different Temperatures for different weld regions

After completing the experiment for pH 5, the results of all three different temperatures of 27°C, 40°C and 60°C are the plotted together to compare the corrosion rate between them as shown in Figure 25. From the results of LPR weld corrosion sweep, it is shown for all three of the temperatures that the weld metal has the highest corrosion rate followed by the heat affected zone and finally the base metal for all three temperatures.

The corrosion rate for the HAZ 1 region is observed to be higher than HAZ 2.This may be due to the difference in the microstructure of the HAZ region which is affected by the temperature distribution during the welding process.HAZ can be divided to three zones of coarse grain zone, followed by the intermediate grain zone and finally the fine grain zone therefore there might be differences between the samples done which have affected the corrosion rates obtained. However, both of the base metals give corrosion rates which do not differ much from each other.

Apart from that, the effect of temperature is also significant in the result obtained. It is shown above in Figure 25 that the corrosion rates for each of the weld regions increases as the temperature increases but similar trends of the three different regions is obtained. Temperature increases the rate of almost the chemical reactions therefore increasing the corrosion rate of the samples. Experiments were then continued for the second parameter which is for pH 6 at the temperature of 27, 40 and 60 ˚C.

4.4.3 Results for pH 6 at 27, 40 and 60 ˚C.

Table 6 shows the self corrosion rates from the linear polarization weld corrosion sweep at pH 6 for 90 minutes immersion in CO_2 saturated 3% NaCl solution at 27˚C.

Table 6: Self-Corrosion rate for blank pH 6 at 27 ˚C (CR-mm/yr)

No	**Z1**	**Z2**	**Z3**	**Z4**	**Z5**
	BM1	**HAZ1**	**WM**	**HAZ2**	**BM2**
1	1.39	1.85	1.88	1.86	1.23
2	1.48	1.85	1.84	1.85	1.24
3	1.41	1.85	1.86	1.89	1.27
4	1.46	1.88	1.90	1.86	1.16
5	1.39	1.91	1.81	1.85	1.22
Average	**1.43**	**1.87**	**1.86**	**1.86**	**1.22**

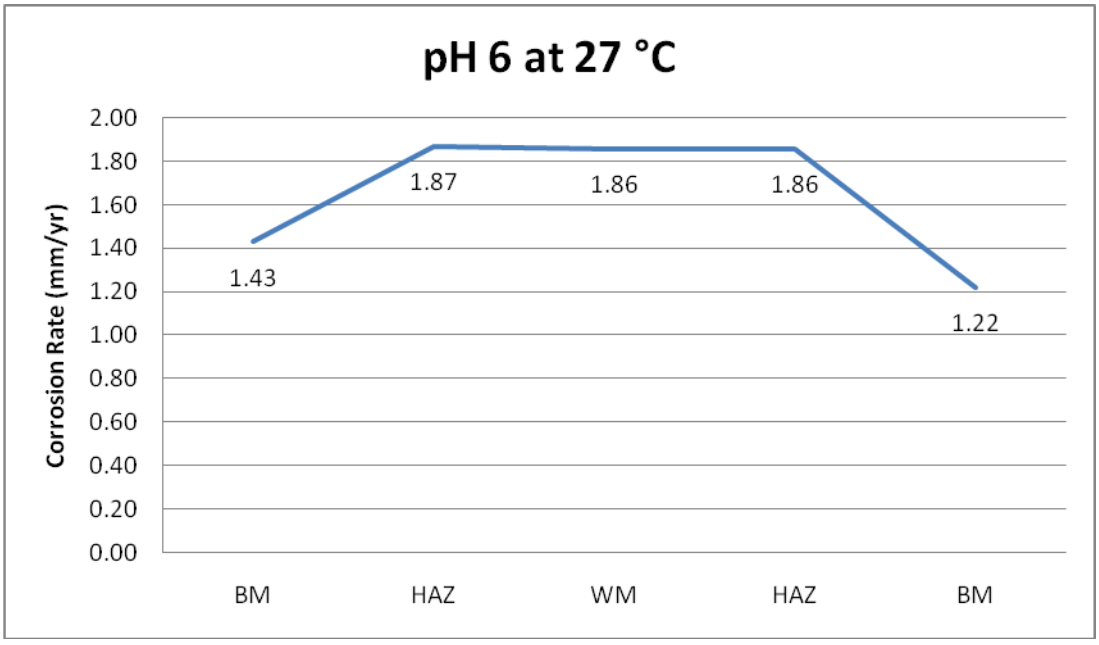

Figure 26: Corrosion Rate for different weld regions, pH 6 at 27 ˚C

Different trends of corrosion rates were obtained for pH 6 compared to the experiment conducted at pH 5.It is shown above from the initial experiment at

ambient temperature that the corrosion rate for HAZ 1 is the highest with 1.87 mm/yr followed by HAZ2 and BM2 both giving results of 1.86 mm/yr and finally the base metal, BM1 with 1.43mm/yr and BM2 with 1.22 mm/yr. It is seen that the weld metal and the HAZ regions are the most anodic compared to the base metal although there are not much difference between its corrosion rates. The base metal regions give lower corrosion rates thus showing that it is less susceptible to the corrosion process.

Table 7 shows the self corrosion rates from the linear polarization weld corrosion sweep at pH 6 for 90 minutes immersion in CO_2 saturated 3% NaCl solution at 40˚C.

Table 7: Self-Corrosion rate for blank pH 6 at 40 ˚C (CR-mm/yr)

No	**Z1**	**Z2**	**Z3**	**Z4**	**Z5**
	BM1	**HAZ1**	**WM**	**HAZ2**	**BM2**
1	1.42	2.37	2.11	2.25	1.43
2	1.48	2.57	2.08	2.24	2.06
3	1.27	2.23	1.91	2.23	2.10
4	1.62	2.04	1.98	2.63	2.08
5	1.62	2.13	1.86	2.33	2.18
Average	**1.48**	**2.27**	**1.99**	**2.33**	**1.97**

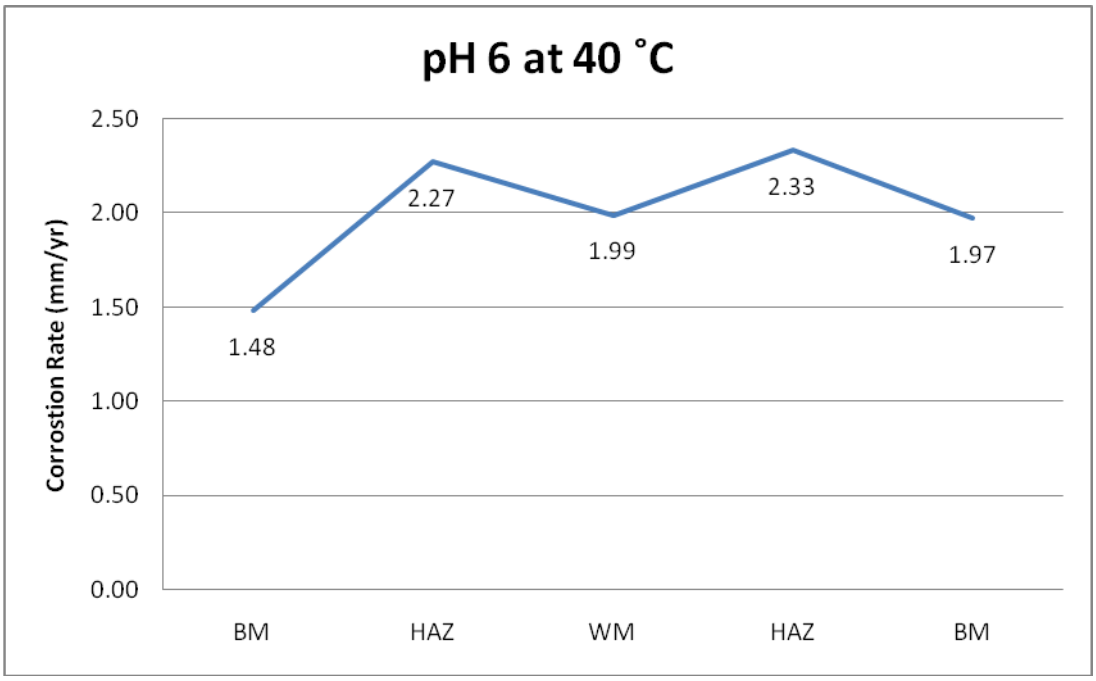

Figure 27: Corrosion Rate for different weld regions, pH 6 40 ˚C

For pH 6 at 40 ˚C the irregular trends of the corrosion rates is as shown in Figure 27. The corrosion rate of HAZ1 is the highest with 2.27 mm/yr followed by HAZ 1 with 2.33 mm/yr. The weld metal at this temperature gives lower corrosion rate compared to the HAZs with 1.99 mm/yr. However, the corrosion rates of the base metals are less than the HAZs and also the weld metal, BM1 with 1.48mm/yr and BM2 with 1.97 mm/yr. There are minor differences of the corrosion rates for the base metal might have been caused by the slight differences of the microstructure of the base metal.

Table 8 shows the self corrosion rates from the linear polarization weld corrosion sweep at pH 6 for 90 minutes immersion in CO_2 saturated 3% NaCl solution at 60˚C.

Table 8: Self-Corrosion rate for blank pH 6 at 60 ˚C (CR-mm/yr)

No	**Z1**	**Z2**	**Z3**	**Z4**	**Z5**
	BM1	**HAZ1**	**WM**	**HAZ2**	**BM2**
1	2.60	3.24	3.24	3.72	2.78
2	2.65	3.12	2.90	3.53	2.30
3	2.21	3.25	3.11	3.67	2.33
4	2.45	3.06	3.03	3.19	2.20
5	2.09	3.11	3.13	3.45	2.09
Average	**2.40**	**3.15**	**3.08**	**3.51**	**2.34**

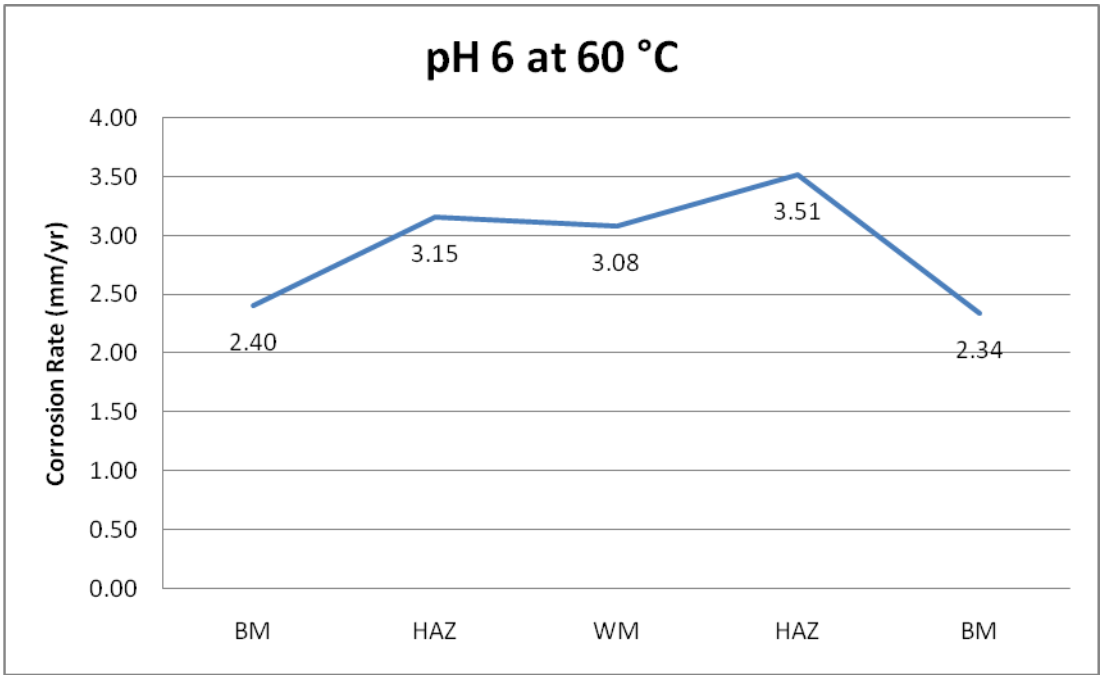

Figure 28: Corrosion Rate for different weld regions, pH 6 at 60 ˚C

The experiment done at 60 ˚C shows that HAZ2 has the highest corrosion rate of all with 3.51 mm/yr, followed by HAZ1 with 3.15 mm/yr and weld metal with

3.08mm/yr. The base metals gave the lowest corrosion rate, BM1 with 2.40 mm/yr and BM2 with 2.34 mm/yr. It can be seen that there are still irregular trends of the corrosion rate for each of the regions compared to the earlier results obtained from pH 5 but at 60˚C, however the HAZs and also the weld metal are obtained to be more anodic compared to both of the base metal. Comparison of the corrosion rates for the temperatures of 27, 40 and 60 ˚C for pH 6 is shown in Figure 29.

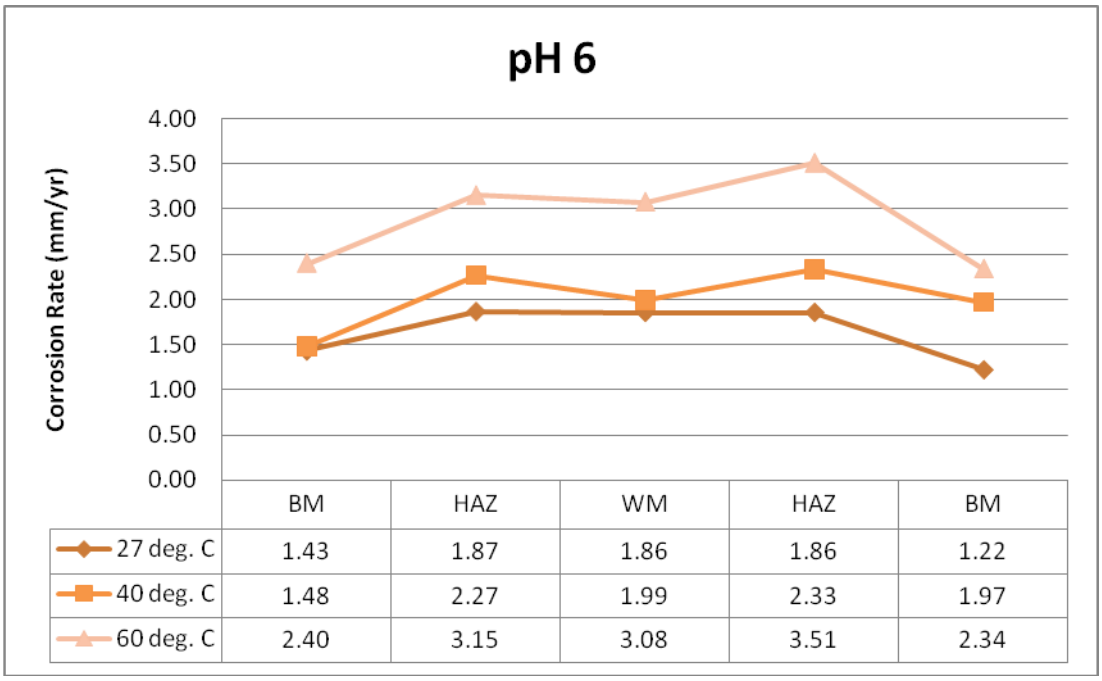

	BM	HAZ	WM	HAZ	BM
27 deg. C	1.43	1.87	1.86	1.86	1.22
40 deg. C	1.48	2.27	1.99	2.33	1.97
60 deg. C	2.40	3.15	3.08	3.51	2.34

Figure 29: Comparison of Corrosion Rate for pH 6 at Different Temperatures for different weld regions

The figure above shows that the trends of the corrosion rates are very different to the corrosion rate trends of the experiment done at pH 5.Compared to the earlier results from pH 5 where the weld metal region has the highest corrosion rates at 27, 40 and 60 ˚C, results from pH 6 shows that the HAZs region has higher corrosion rates compared to the weld metal. Even though the trends are different for the different pH, it is seen that the weld metal and the HAZ regions are more anodic to the base metal for all of the results obtained. Therefore the result indicates that the HAZ and weld region are more susceptible corrosion, exposing the welded pipelines to low area of anode to the large area of cathode which will lead to preferential weld corrosion and is highly undesirable.

Apart from that, the irregular trends of pH 6 at different temperature is inconclusive and further study on the effect of pH to the corrosion rate needs to be done to clarify this phenomena and also the effect of the pH to the different microstructures of the weld.

However, the effect of temperature still can be observed here which gives highest value of corrosion rate at the highest temperature of 60 ˚C therefore confirms the influence of the temperature to the value of the corrosion rate. This occur due to the fact that temperature increases the rate of almost all chemical reactions hence the increased temperature increases the oxidizing power which then causes an increase in the corrosion rate of the weld regions.

From the LPR weld corrosion sweep test, it is obtained that different regions of the weld metal which have different type of microstructures due to the temperature distribution or duration of the welding gives different individual corrosion rates at different temperatures and pH. Although different trends are obtained for different pH, the result still shows that the regions of weld metal and heat-affected zone are more anodic and susceptible to corrosion compared to the base metal. This is a major concern especially because of the unfavourable area ratio which consists of a large cathode and a small anode which will then cause preferential weld corrosion especially at the weld region itself.

4.4 Galvanic Current Density Results

The galvanic current density measurement was done at only ambient temperature of 27 ˚C since the corrosion rate trend is the same at all three temperatures based on the result earlier for pH 5.The readings are recorded for every 5 seconds for a period of 2 hours simultaneously for the coupled weld metal & HAZ and also the Base metal & HAZ. The results obtained are shown in Figure 30.

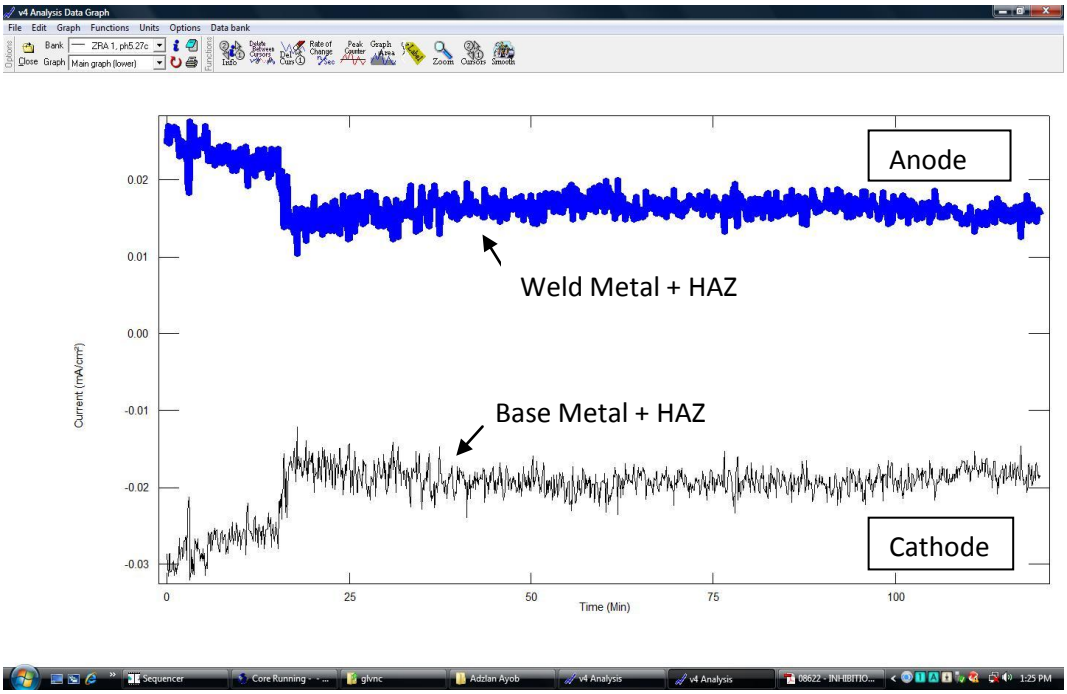

Figure 30: Galvanic Current Density Measurement at pH 5, 27 ˚C

Based on the result of the galvanic current density, the coupled weld metal and HAZ were both anodic throughout the test with the current density values above zero in the anode region while the coupled base metal and HAZ were both cathodic with values below zero in the cathode region. In general, the magnitude of the current was the highest for the coupled Weld Metal and HAZ. This indicates that in a welded pipeline, the region of HAZ and Weld metal is the most susceptible to corrosion. Table 9 shows the galvanic current density value obtained from the experiment.

Table 9: Galvanic Current Density for Coupled Sample

Galvanic Coupled Sample	**Galvanic Current Density ($mA.cm^{-2}$)**
Weld Metal+HAZ	0.015
HAZ+Base Metal	-0.020

The individual currents from the coupled samples were established from the following relationship:

$$\mathbf{I_{BM} + I_{HAZ} + I_{WM} = 0}$$

From the relationship, the individual current density is obtained as shown in Table 10.

Table 10: Galvanic Current Density and Galvanic Corrosion Rate of Different Weld Regions

Weld Region	**Galvanic Current Density ($mA.cm^{-2}$)**	**Galvanic Corrosion Rate ($mm.yr^{-1}$)**
Base Metal	-0.015	-0.174
HAZ	-0.005	-0.058
Weld Metal	0.020	0.232

The total corrosion rate of each weld region can be considered to be the sum of its self-corrosion (pH 5) and galvanic corrosion rates. The average self-corrosion rates were taken for the HAZ and also base metal region. The total corrosion rate is as shown in Table 11.

Table 11: The Total Corrosion Rate of Different Weld Regions

Weld Region	**Self-Corrosion Rate ($mm.yr^{-1}$)**	**Galvanic Corrosion Rate ($mm.yr^{-1}$)**	**Total Corrosion Rate ($mm.yr^{-1}$)**
Base Metal	1.95	-0.174	1.776
HAZ	2.89	-0.058	2.832
Weld Metal	3.20	0.232	3.432

From Table 11, it can be seen that the galvanic contribution was much smaller than the self-corrosion rate of each region. This is because carbon-steel is inherently susceptible to high-self corrosion rates in CO2 environments, whereas the small compositional and microstructural difference between the weld regions would have not caused large galvanic differences.

Furthermore the large cathodic area with the lower current density of the base metal to the anodic area of the weld metal and HAZ with higher current density may increase the rate or intensity of the corrosion at the weld region. Preferential weld

corrosion will surely occur in welded pipelines therefore further study has to be done in order to overcome this problem.

CHAPTER 5

CONCLUSION AND RECOMMENDATIONS

Microstructures from the sample of the welded pipeline showed the different microstructure at different regions for the weldments which is the unaffected base metal, Heat-affected Zone and the weld metal. Vickers hardness test was done to obtain the hardness of the sample at different zones to indicate that there are differences of the mechanical properties due to the difference of microstructure. Weld metal gave the highest hardness value due to the acicular ferrite form of the grains.

Results from the experiment indicated the microstructures do affect the corrosion rate of the weld metal at different regions. Results from pH 5 at different temperatures gave similar trends of highest corrosion rates at the weld metal region followed by the HAZ and finally the base metal region, having the weld metal and also the HAZ to be more susceptible to corrosion compared to the unaffected base metal. The affect of different pH was not conclusive due to the irregular trends obtained from the experiment done for pH 6.The results from pH 6 however still indicated that the HAZ and also the weld metal region are more anodic compared to the base metal. Other than that, it is also shown from the results that corrosion is more severe at higher temperatures due to the acceleration of the chemical reactions.

Finally, the galvanic current density measurement was done on the sample for pH 5 at room temperature to monitor the affect of galvanic corrosion to the weld sample. From the result it is concluded that the coupled weld metal and HAZ are more anodic compared to the coupled base metal and HAZ. This will result in accelerated corrosion of the weld region due to the unbalance ratio of anodic and

cathodic area. The galvanic corrosion rate was found to be small since there are only slight differences between the microstructures of the same type of metal.

With the result obtain and the analysis done on the affect of different microstructure at the different regions of the weld pipeline to the individual corrosion rates and also the galvanic current measurement, it is concluded that the objectives of this research are met. Based on the result it is known that welded joints are more anodic compared to the rest of the pipe at different pH and temperatures. Therefore it is necessary for the prediction model to consider the welded joints in their prediction.

5.1 Recommendations

Upon completing the research for this project, it is known that there are still areas where by further studies need to be done in order to understand more on the behaviour of the weld regions to the different pH based on the inconclusive result obtained from the experiment at pH 6 done.

However, the need to control the corrosion rate of the weld metal region which is accelerated by the large cathode area of unaffected base metal is similarly important to prevent failure for the pipelines being used in the industry. Therefore the study on the corrosion prevention method for the preferential weld corrosion can be done as a continuation of this project.

REFERENCES

[1]Lee, C.M., Bond, S. And Woollin, P. 2005. Preferential Weld Corrosion*:Effects of Weldment Microstructure and Composition*, Corrosion 2005, Paper No. 05277, Houston, TX: NACE International, 2005.

[2]Bond, S. 1999. *Risk of Preferential Weldment Corrosion of Ferritic Steels in CO_2 Containing Environtments* Corrosion 2005, Proposal No. GP/MAT/1165-1, CopyrighTWI, 1999.

[3]Clover, D., Kinsella, B., Pejcic, B. And De Marco,R. 2005.*The Influence of Microstructure on the Corrosion Rate of Various Carbon Steels* Journal of Applied Chemistry (2005) 35:139-149

[4]Lopez, D.A., Perez, T. And Simison, S.N. 2003.*The Influence of Microstructure and Chemical Composition of Carbon and Low Alloy Steels In CO_2 Corrosion.A State-of-the-art appraisal* Materials and Design 24 (2003) 561-575

[5]Turgoose, S., Palmer, J.W. And Dicken, G.E. 2005. Preferential Weld Corrosion of 1% Ni Welds*:Effects of solution conductivity and corrosion inhibitors,* Corrosion 2005, Paper No. 05275, Houston, TX: NACE International, 2005.

[6]Gulbrandsen, E. And Dugstad, A. 2005.*Corrosion Loop Studies of Preferential Weld Corrosion and its Inhibition in CO_2 Environments,* Corrosion 2005, Paper No. 05276, Houston, TX: NACE International, 2005.

[7]Andreassen,R. And Enerhaug,J. 1997.*On the effect of Microstructure in CO_2 corrosion of Carbon Steel Welds* Advances in Corrosion Control and Materials in Oil and Gas Production. EFC publications No. 26-1999, pp 77-83

[8]Kermani,M.B. And Smith,L.M. 1997. *CO_2 Corrosion Control in Oil and Gas Production*. EFC publications.

[9]Kalpakjian,S. And Schmid, S. 2006.*Manufacturing Engineering and Technology*,Fifth Edition,Singapore,Pearson Prentice Hall.

[10]Wahid, A., Olson, D.L., Matlock, D.K. and Cross, C.E.1993.Corrosion of Weldments,*Welding,Brazing, and Soldering,*Vol 6,ASM Handbook,*ASM International*

[11]Unknown Author.8 May 2002 <http://www.gowelding.com/met/carbon.htm>

[12]Askeland,Donald. And P.PHule,Pradeep. 2003. *The Science and Engineering of Materials*, Fourth Edition, United States, Thomson Learning,Inc.

[13]Alawadhi, K., Robinson, M.,Chalmers, A. And Winning, I.G. 2008 .*Inhibition of Weld Corrosion in Flowing Brines Containing Carbon Dioxide*, Corrosion 2008, Paper No. 08622, Houston, TX: NACE International, 2008.

[14]Annual Book of ASTM Standard, Vol 03.02: *ASTM G 59, Standard Practice for Conducting Potentiodynamic Polarization Resistance Measurements.*

[15]Annual Book of ASTM Standard, Vol 03.02: *ASTM G 102 – 89, Standard Practice for Calculation of Corrosion Rates and Related Information from Electrochemical Measurement.*

[16]Annual Book of ASTM Standard, Vol 03.02: *ASTM G 1, Standard Practice for Preparing, Cleaning, and Evaluating Corrosion Test Specimens* .

APPENDICES